Downstream Evaluation on Diffusion Metrics for Susceptibility Artifact Correction via Complex Forward-Distortion Network

Abdallah Zaid Alkilani[1,2], Atakan Topcu[1,2], Tolga Çukur[1,2,3], and Emine Ulku Saritas[1,2]

[1]Department of Electrical and Electronics Engineering, Bilkent University, Ankara, Turkey, [2]National Magnetic Resonance Research Center (UMRAM), Bilkent University, Ankara, Turkey, [3]Neuroscience Graduate Program, Bilkent University, Ankara, Turkey

---

0. Summary

This study examines a deep learning method for EPI susceptibility correction that merges physics-constrained learning with phase-injected formulation and two-step training, and assesses its impact on diffusion metrics. It offers quick and effective correction, suitable for clinical and research use.

---

1. Introduction

Diffusion MRI (dMRI) enhances our understanding of the brain's fiber structure and connectome, with its efficacy hinging on data-intensive multi-shell sampling [1-5]. Derived metrics from dMRI enable visualization and assessment of the integrity of white matter pathways [6,7].

Echo planar imaging (EPI) is a rapid imaging sequence that is preferred for dMRI due to its motion robustness; yet, EPI suffers from susceptibility artifacts that compromise resultant diffusion-weighted image (DWI) quality [8,9], obligating correction for accurate quantitative analysis [10]. Typically, reversed-phase-encode (reversed-PE) methods are used to correct for these artifacts in EPI images [11]. However, traditional correction methods are computationally demanding, limiting practicality in clinical settings.

We recently introduced complex Forward-Distortion Network (compFD-Net) for unsupervised susceptibility artifact correction in EPI images via a phase-injection formulation [12,13]. comFD-Net's performance was proven effective for high SNR b0 images. However, when the compFD-Net model trained on b0 images was zero-shot transferred to process low-SNR b>0 images, it performs suboptimally. In this work, we propose an extended method compFD-Net+ that improves correction performance on multi-shell dMRI data via a two-step training approach. In particular, we propose to pre-train compFD-Net+ on relatively high-SNR b0 images to boost initial learning, and then to fine-tune it on b>0 images to increase specialization to image features at higher *b*-values. Downstream evaluations on dMRI metrics demonstrate the efficiency of this approach, as well as its computational advantage with respect to classical correction techniques such as TOPUP.

2. Methods

Classical Correction Approach

Field-map based correction techniques for susceptibility artifacts use reversed-PE images, assuming opposite distortions along the PE direction and directly correcting the images using an estimated field [14]. In this study, we employ FSL's TOPUP as our reference method, regarded as a gold-standard for EPI distortion correction based on field estimates derived from reversed-PE images [11,15].

Dataset & Learning Procedures

We used randomly selected, unprocessed dMRI data from the Human Connectome Project's 1200 Subjects Data Release [16]. The gradient tables included 89 diffusion-weighting directions with 6 interspersed b0 acquisitions. The diffusion-weighting directions were uniformly distributed over three q-space shells with b=(1000, 2000, 3000) s mm^{-2}.
A (42, 4, 8)-subject split was used for training, validation, and testing. The proposed compFD-Net+ was pre-trained on b0 images from 42 training subjects, and then fine-tuned on b>0 images from a subset of 12 training subjects. This two-step training is driven by the notably higher SNR of b0 images compared to b>0 images. Meanwhile, compFD-Net was exclusively trained on b0 images from 42 training subjects.

Evaluation on Diffusion Metrics

The downstream effects of susceptibility artifact correction with the proposed technique are evaluated for the following diffusion metrics: Fractional anisotropy (FA) and mean diffusivity (MD) metrics from diffusion tensor imaging (DTI) [1,17]; Orientation dispersion index (ODI) and intracellular volume fraction (ICVF) metrics from NODDI [18]; Apparent fiber density (AFD) and number of fiber orientations (nuFO) metrics from MT-CSD [6,19]. FA and MD were derived using DIPY [20], ODI and ICVF using AMICO [21], and AFD and nuFO using MRTrix3 [22]. TOPUP correction was applied for reference, and brain masks were derived from TOPUP's b0 images with FSL's brain extraction tool [23].

3. Results

The diffusion metrics for compFD-Net, the proposed compFD-Net+, and TOPUP were calculated from their respective DWIs after susceptibility correction. On average, TOPUP required ~51 minutes to compute the displacement field and ~6 seconds for correcting each volume afterwards, with a total correction time of ~60 minutes per subject. In contrast, correcting a single volume using compFD-Net or compFD-Net+ took ~8 seconds, reducing the total correction time to ~13 minutes per subject.

The dMRI metrics for a representative slice are shown in Figure 2. Visually, compFD-Net+ demonstrates higher consistency to TOPUP results than compFD-Net. The image quality assessments in Table 1 and 2 demonstrate the superiority of compFD-Net+ over compFD-Net across DWIs from different *b*-values and diffusion metrics, respectively. Improvements for compFD-Net+ are consistently observed across all evaluations.

4. Discussion and Conclusion

The results show that compFD-Net+ delivers high-grade correction of multi-shell dMRI data across *b*-values and yields accurate dMRI metrics. The two-step training approach extends the physics-constrained phase-injected complex formulation to boost susceptibility correction quality and enhance model generalizability.compFD-Net+ maintains fidelity while rapidly performing correction, demonstrating potential in clinical and research settings.

References

1. D. L. Bihan, J. F. Mangin, C. Poupon, C. Clark, S. Pappatà, N. Molko *et al.*, “Diffusion tensor imaging: Concepts and applications,” *J. Magn. Reson. Imag.*, vol. 13, 2001.
2. G. Tran and Y. Shi, “Fiber orientation and compartment parameter estimation from multi-shell diffusion imaging,” *IEEE Trans. Med. Imag.*, vol. 34, pp. 2320–2332, 2015.
3. Y. Shi and A. Toga, “Connectome imaging for mapping human brain pathways,” *Molecular Psychiatry*, vol. 22, pp. 1230 – 1240, 2017.
4. J. Jensen, G. Glenn, and J. Helpern, “Fiber ball imaging,” *NeuroImage*, vol. 124, pp. 824–833, 2016.
5. D. V. Olson, V. E. Arpinar, and L. Muftuler, “Optimization of q-space sampling for mean apparent propagator mri metrics using a genetic algorithm,” *NeuroImage*, vol. 199, pp. 237–244, 2019.
6. D. Raffelt, J.-D. Tournier, S. Rose, G. R. Ridgway, R. Henderson, S. Crozier *et al.*, “Apparent fibre density: A novel measure for the analysis of diffusion-weighted magnetic resonance images,” *NeuroImage*, vol. 59, no. 4, pp. 3976–3994, 2012.
7. D. Jones, “Studying connections in the living human brain with diffusion MRI,” *Cortex*, vol. 44, no. 8, pp. 936–952, 2008.
8. S. J. Holdsworth and R. Bammer, “Magnetic resonance imaging techniques: fMRI, DWI, and PWI,” *Semin. Neurol.*, vol. 28, no. 4, pp. 395–406, 2008.
9. P. Mansfield, “Multi-planar image formation using NMR spin echoes,” *J. phys.*, vol. 10, no. 3, pp. L55–L58, 1977.
10. J.-D. Tournier, S. Mori, and A. Leemans, “Diffusion tensor imaging and beyond,” *Magn. Reson. Med.*, vol. 65, no. 6, pp. 1532–1556, 2011.
11. S. M. Smith *et al.*, “Advances in functional and structural MR image analysis and implementation as FSL,” *Neuroimage*, vol. 23 Suppl 1, pp. S208-19, 2004.
12. A. Zaid Alkilani, T. Çukur, and E. U. Saritas, "FD-Net: An unsupervised deep forward-distortion model for susceptibility artifact correction in EPI," *Magn. Reson. Med.*, vol. 91, no. 1, pp. 280–296, 2024.

13. A. Zaid Alkilani, T. Çukur, and E. U. Saritas, “A Phase-Injected Complex Forward-Distortion Approach for Deep Unsupervised Correction of Susceptibility Artifacts in EPI,” *Proc. of the 32nd Annu. Meet. of ISMRM*, Singapore, Singapore, 2024, p. 1370.
14. D. Holland, J. M. Kuperman, and A. M. Dale, “Efficient correction of inhomogeneous static magnetic field-induced distortion in Echo Planar Imaging,” *Neuroimage*, vol. 50, no. 1, pp. 175–183, 2010.
15. J. L. R. Andersson, S. Skare, and J. Ashburner, “How to correct susceptibility distortions in spin-echo echo-planar images: application to diffusion tensor imaging,” *Neuroimage*, vol. 20, no. 2, pp. 870–888, 2003.
16. D. C. Van Essen, S. M. Smith, D. M. Barch, T. E. J. Behrens, E. Yacoub, and K. Ugurbil, “The WU-Minn Human Connectome Project: An overview,” *Neuroimage*, vol. 80, pp. 62–79, 2013.
17. E. Özarslan and T. H. Mareci, “Generalized diffusion tensor imaging and analytical relationships between diffusion tensor imaging and high angular resolution diffusion imaging,” *Magn. Reson. Med.*, vol. 50, no. 5, p. 955–965, 2003.
18. H. Zhang, T. Schneider, C. A. Wheeler-Kingshott, and D. C. Alexander, “Noddi: Practical in vivo neurite orientation dispersion and density imaging of the human brain,” *NeuroImage*, vol. 61, no. 4, p. 1000–1016, 2012.
19. B. Jeurissen, J.-D. Tournier, T. Dhollander, A. Connelly, and J. Sijbers, “Multi-tissue constrained spherical deconvolution for improved analysis of multi-shell diffusion mri data,” *NeuroImage*, vol. 103, p. 411–426, 2014.
20. E. Garyfallidis *et al.*, “Dipy, a library for the analysis of diffusion MRI data,” *Front. Neuroinform.*, vol. 8, p. 8, 2014.
21. A. Daducci, E. J. Canales-Rodríguez, H. Zhang, T. B. Dyrby, D. C. Alexander, and J.-P. Thiran, “Accelerated Microstructure Imaging via Convex Optimization (AMICO) from diffusion MRI data,” *Neuroimage*, vol. 105, pp. 32–44, 2015.
22. J.-D. Tournier *et al.*, “MRtrix3: A fast, flexible and open software framework for medical image processing and visualisation,” *Neuroimage*, vol. 202, no. 116137, p. 116137, 2019.
23. S. M. Smith, “Fast robust automated brain extraction,” *Hum. Brain Mapp.*, vol. 17, no. 3, pp. 143–155, 2002.

Figures

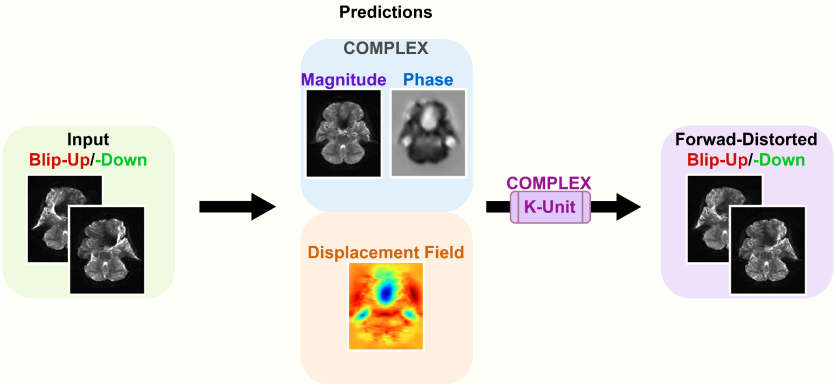

Figure 1. Overview of the compFD-Net+ architecture. The input EPI blip-up and blip-down (i.e., reversed-PE) images are used to predict the susceptibility-induced displacement field and the underlying anatomically correct image as a complex-valued image (represented as magnitude and phase images). The corrected complex-valued image is forward distorted with the displacement field via the complex K-Unit, and the forward-distorted images are used to enforce fidelity to the input EPI blip-up and blip-down images.

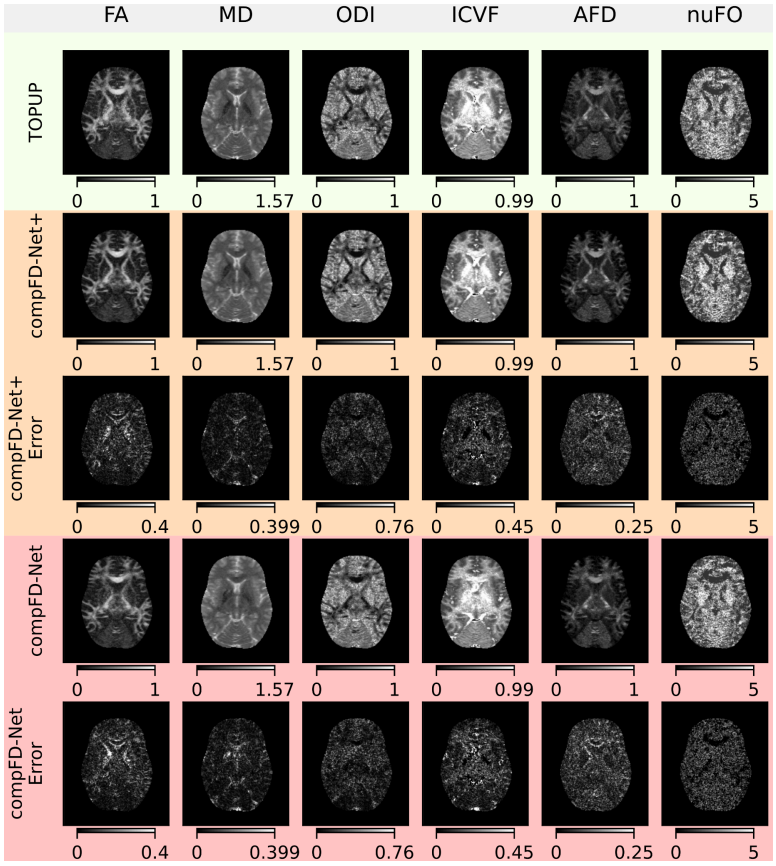

Figure 2. Diffusion metrics from a representative slice. Both the proposed compFD-Net+ and compFD-Net are compared to TOPUP via absolute error maps. MD is measured in units of 10^{-3} mm^2 s^{-1}. Note that nuFO is a discrete map.

b-value (s/mm^2)	Model	PSNR [dB]	SSIM [%]
0	**compFD-Net+**	**33.09 (3.94)**	**94.27 (10.62)**
	compFD-Net	31.61 (3.48)	89.52 (10.05)
1000	**compFD-Net+**	**29.24 (2.41)**	**74.26 (11.70)**
	compFD-Net	27.93 (2.69)	67.49 (12.96)
2000	**compFD-Net+**	**27.65 (2.20)**	**62.08 (11.79)**
	compFD-Net	26.46 (2.47)	54.75 (13.18)
3000	**compFD-Net+**	**26.97 (2.13)**	**54.60 (11.16)**
	compFD-Net	25.87 (2.43)	47.31 (13.06)

Table 1. Image quality assessment comparison across DWIs with different *b*-values for the proposed compFD-Net+ and compFD-Net. TOPUP results are taken as reference. PSNR (units: dB) and SSIM (percentage) are provided as mean and standard deviation (in parentheses) across all slices from the test subjects.

Diffusion Metric	Model	PSNR [dB]	SSIM [%]
FA	**compFD-Net+**	**27.55 (4.70)**	**93.05 (5.40)**
	compFD-Net	26.17 (4.70)	90.80 (6.30)
MD	**compFD-Net+**	**32.88 (9.70)**	**96.21 (2.90)**
	compFD-Net	31.66 (9.60)	94.48 (3.60)
ODI	**compFD-Net+**	**24.06 (4.70)**	**90.52 (6.70)**
	compFD-Net	22.97 (4.80)	88.03 (7.70)
ICVF	**compFD-Net+**	**23.67 (4.60)**	**91.24 (5.40)**
	compFD-Net	22.64 (4.70)	88.65 (6.50)
AFD	**compFD-Net+**	**28.92 (4.00)**	**92.77 (5.40)**
	compFD-Net	27.69 (4.00)	90.78 (6.10)
NuFO	**compFD-Net+**	**19.52 (4.70)**	**83.31 (9.90)**
	compFD-Net	19.07 (4.80)	81.61 (10.70)

Table 2. Image quality assessment comparison across diffusion metrics for the proposed compFD-Net+ and compFD-Net. TOPUP results are taken as reference. PSNR (units: dB) and SSIM (percentage) are provided as mean and standard deviation (in parentheses) across all slices from the test subjects.